Biophysical Reviews (2018) 10:709–719
https://doi.org/10.1007/s12551-017-0390-3

REVIEW

# Thermodynamics of interaction of ionic liquids with lipid monolayer

G. Bhattacharya[1] · S. Mitra[1] · P. Mandal[1] · S. Dutta[2] · R. P. Giri[3] · S. K. Ghosh[1]

Received: 25 September 2017 / Accepted: 13 December 2017 / Published online: 5 January 2018


## Abstract

Understanding the interaction of ionic liquids with cellular membrane becomes utterly important to comprehend the activities of these liquids in living organisms. Lipid monolayer formed at the air–water interface is employed as a model system to follow this interaction by investigating important thermodynamic parameters. The penetration kinetics of the imidazolium-based ionic liquid 1-decyl-3-methylimidazolium tetrafluoroborate ([DMIM][BF4]) into the zwitterionic 1,2-dipalmitoyl-sn-glycero-3-phosphocholine (DPPC) lipid layer is found to follow the Boltzmann-like equation that reveals the characteristic time constant which is observed to be the function of initial surface pressure. The enthalpy and entropy calculated from temperature-dependent pressure–area isotherms of the monolayer show that the added ionic liquids bring about a disordering effect in the lipid film. The change in Gibbs free energy indicates that an ionic liquid with longer chain has a far greater disordering effect compared to an ionic liquid with shorter chain. The differential scanning calorimetric measurement on a multilamellar vesicle system shows the main phase transition temperature to shift to a lower value, which, again, indicates the disordering effect of the ionic liquid on lipid membrane. All these studies fundamentally point out that, when ionic liquids interact with lipid molecules, the self-assembled structure of a cellular membrane gets perturbed, which may be the mechanism of these molecules having adverse effects on living organisms.

**Keywords** Cellular membrane · Ionic liquids (ILs) · Lipid monolayer · Thermodynamics

## Introduction

Cellular membrane is a bilayer of lipids with proteins, cholesterol, etc. embedded within it. This membrane not only provides the protective boundary to a cell but also executes and controls many physiological functions, such as endocytosis–exocytosis processes and cell signaling (Lombard 2014). Any perturbation in the natural structure of this membrane due to interaction with an external molecule may have an impact on these functions. Ionic liquids (ILs) are such foreign molecules which have been reported to show adverse effects on living organisms (Docherty and Kulpa 2005). These molecules are found to be toxic to many of the bacteria and fungi (Babalola 1998; Li et al. 1998; Kelman et al. 2001). These are organic salts with low melting point, generally below 100 °C (Hallett and Welton 2011). These molecules have wide industrial application, as they replace the common organic solvents (Rogers et al. 2009). As they have low vapor pressure, they do not pollute air. However, because of their high thermal stability and non-biodegradability, they have become accumulated in aqueous bodies, causing water pollution (Gorman-Lewis and Fein 2004) and kill many eco-friendly microorganisms (Yu and Nie 2011; Kulacki and Lamberti 2008). On the other hand, there are controlled and selective uses of these molecules in the development of anticancer, antimicrobial, and antifungal medicines (Smiglak et al. 2014). A series of different physical and chemical characterizations and several bioassays are followed in order to study the possible cytotoxicity of ILs. For this purpose, the interaction of ILs with different cell-mimicking model biological systems consisting of

This article is part of a Special Issue on 'Ionic Liquids and Biomolecules' edited by Antonio Benedetto and Hans-Joachim Galla.

✉ S. K. Ghosh
sajal.ghosh@snu.edu.in

[1] Department of Physics, School of Natural Sciences, Shiv Nadar University, NH-91, Tehsil Dadri, G. B. Nagar, Uttar Pradesh 201314, India

[2] Department of Chemistry, School of Natural Sciences, Shiv Nadar University, NH-91, Tehsil Dadri, G. B. Nagar, Uttar Pradesh 201314, India

[3] Saha Institute of Nuclear Physics, Bidhannagar, Kolkata 700064, India

nucleic acid and phospholipid bilayers have been investigated (Laszlo and Compton 2002; DiCarlo et al. 2006; Ranke et al. 2007). Disruption and deformation of cellular organization by ILs have been monitored using transmission electron, atomic force, and polarization optical microscopy techniques, along with the quartz crystal microbalance technique (Byrne and Angell 2009; Kalhor et al. 2009; Evans 2008). In addition to this, various molecular dynamic (MD) studies have also been executed to understand the potential cytotoxicity (Yoo et al. 2014). MD simulations indicate that the self-assembly of the cellular membrane suffers a strong physical disruption that may interfere with cell signaling processes, leading to lysing of a cell (Yoo et al. 2016; Bingham and Ballone 2012; Lim et al. 2014). There are many reports of severe and extended cytotoxicity of imidazolium-based ILs; researchers have even established the adverse effect on mammalian as well as human cell lines (Frade et al. 2007; Kumar et al. 2009; Ranke et al. 2007). Recent reports have suggested the activities of these molecules to be related to their disruptive effects on the self-assembled structure of cellular membrane (Yoo et al. 2014; Mikkola et al. 2015; Kontro et al. 2016; Drücker et al. 2017). X-ray and neutron scattering studies have quantified these effects on lipid bilayers formed on planar surfaces (Benedetto et al. 2014; Bhattacharya et al. 2017). Further, MD simulations have shown a considerable effect of these molecules on the dynamic behavior of lipids in the plane of a bilayer (Benedetto et al. 2015). Quasielastic neutron scattering (QENS) experiments have shown that the long-range lateral motion and localized internal motions of lipid molecules in unilamellar vesicles are enhanced due to the presence of long-chain imidazolium-based ILs (Sharma et al. 2017).

Even though there are many in vivo and in vitro experiments using various techniques to investigate the effects of ILs on cellular membranes, there are not enough thermodynamic measurements to understand the nature of IL–lipid interactions. Thermodynamics is one of the most fundamental disciplines in science that can provide important microscopic information through measuring several macroscopic parameters (Heimburg 2008). In the case of membrane biophysics, this has been used since the 1980s to find out the heat capacity involved in lipid melting (Blume 1983). Especially for understanding the stability of a system, thermodynamic characterizations are important. As we supply heat energy to an ordered system, it changes to a disordered state, which involves changes in the enthalpy and entropy. Another thermodynamic parameter, the excess Gibbs free energy involved in the mixing of two chemical components, could provide us with information about the type of interactions between the components. In a recent paper, Vollhardt and Brezesinski (2016) characterized the phases of 1-monopalmitoyl-rac-glycerol monolayer at the air–water interface by studying the enthalpy and entropy changes associated with the in-plane organization of these molecules. In this work, they have used the two-dimensional Clausius–Clapeyron equation to obtain the change in enthalpy due to the liquid extended to liquid condensed phase transition. Further, from this enthalpy, the change in entropy was calculated. All the values of these thermodynamic parameters satisfy the ordering nature of molecules in liquid condensed (LC) phase compared to that in liquid extended (LE) phase. There are studies showing the phase behavior of lipid molecules in membrane in the presence of other molecules, ranging from inorganic small molecules to organic macromolecules. A series of sodium salts with different anions following the Hofmeister series was taken in the work of Aroti et al. (2004). The effect of these salts on the 1,2-dipalmitoyl-sn-glycero-3-phosphocholine (DPPC) monolayer formed at the air–water interface was studied. The study revealed that these molecules stabilize the LE phase and this stabilization was observed to be a function of salt concentrations and types of anions in the salt. Further, the effect was found to differ in LC phase compared to that of LE phase. The X-ray reflectivity and grazing incidence X-ray diffraction studies by Ghosh et al. (2012) on a similar system but with divalent cation ($Ca^{2+}$) quantified the re-organization of lipid molecules in the monolayer as a consequence of lipid–ion interaction. Petelska and Figaszewski (2011) examined the effect of potassium ion ($K^+$) on the phosphatidylcholine (lecithin, PC) and cholesterol (Ch) monolayer by measuring the excess Gibbs free energy in the presence of $K^+$ ions. The paper reported the formation of stable $PCK^+$ and $ChK^+$ complexes at the air–water interface. The Gibbs free energy of formation of these complexes was found to be negative, which is an indication of the preferred interaction between the molecules. Giehl and coworkers (1999) have used differential scanning calorimetry (DSC) to measure the change in enthalpy to follow the interaction of GM2-activator protein with lipid bilayer and monolayer. From the thermograms measured on unilamellar vesicle of PC lipids, it was clear that the addition of protein decreased the phase transition temperature of the lipids, indicating a decrease in stability of the gel phase. However, such an effect was found to depend on lipid composition. Recently, the interaction of tetrazine (Tz) (a bioimaging analyte) with lipid monolayer was thermodynamically analyzed by Nakahara et al. (2016) by the evaluation of excess Gibbs free energy of the mixing. For all the phospholipids used in the study, the value of this free energy was found to be negative, indicating, again, a preferred mixing and interaction. Contradictorily, the interaction between cholesterol and Tz was found to be negligible. As cholesterol is an important component of developed cellular membrane, there are many thermodynamic studies to characterize the cholesterol–lipid interactions. In order to evaluate this interaction with different lipids and to check the miscibility of lipids with cholesterol, area–pressure isotherms of lipid monolayers of binary systems were measured and, consequently, the excess Gibbs free energies were evaluated. From these free energy data, Jurak (2013) showed that the change in this energy is minimum for the DOPC (1,2-dioleoyl-sn-glycero-3-phosphocholine)–

cholesterol monolayer system, indicating the most stable film, whereas there was hardly any alteration in the DPPG (1,2-dipalmitoyl-sn-glycero-3-phosphorylglycerol)–cholesterol system, suggesting a poor interaction between these molecules. In their monolayer study, Sabatini and co-workers (2008) have shown the disappearance of co-existence of LE–LC phases in the presence of high concentrations of sterols. From the excess Gibbs free energy of mixing, this work established that cholesterol enhances stability in binary monolayer compared to those with ergosterol or lanosterol. Calculating Gibbs free energy from the isotherms of lipid monolayer, Giri et al. (2017a, b) have also shown that the presence of cholesterol in PC lipids has a condensing effect that increases with the increase of concentration of cholesterol.

There are a few recent works where thermodynamic parameters are measured to understand the interaction of ILs with model cellular membranes. Gayet et al. (2011) have prepared multilayer vesicles in IL medium instead of taking water. DSC measurements have revealed the phase transition temperature and enthalpy of transition to be higher in this medium compared to the vesicles in water medium. This was explained as the consequence of the reduction of electrostatic repulsions between the lipid head groups. The study also concluded that the presence of IL in aqueous solution of multilamellar vesicles (MLVs) alters the bilayer structure and stability. In their study on the interaction of choline salts with artificial biological membrane, Weaver et al. (2013) have shown that the ILs with low toxicity have minimal effect on the phase transition temperature of lipids in unilamellar vesicles. The salts that show higher toxicity cause distinct disruption in the phase behavior of lipid molecules. This effect is due to the penetration of these salts into the acyl chains of the phospholipids. Wang et al. (2016) have investigated the effects of imidazolium-based lipid analogs on PC lipid membrane. Both the Gibbs free energy of mixing calculated from PC–imidazolium lipid monolayer and DSC measurements from liposomes of these mixtures indicate the effect to be dependent on the chain length of the imidazolium lipids. While $C_7$–imidazolium lipid shows negligible effect on membrane, $C_{15}$–imidazolium lipid exhibits a rigidification effect. Interestingly, a medium chain length ($C_{11}$) imidazolium lipid showed a disordering effect. In a very recent work, Russo et al. (2017) have observed that the presence of cholesterol in vesicles of phospholipids affects the interaction between ILs and the vesicle. The DSC work showed the binding and infiltration of an phosphonium-based IL to be delayed in the cholesterol-containing vesicles, suggesting the resistive activities of cholesterol.

In this present work, thermodynamic parameters of interaction of imidazolium-based ILs with phosphatidylcholine mono- and bilayers have been investigated systematically. The characteristic time scale of penetration kinetics of these ILs into the lipid monolayer formed at the air–water interface is found to be dependent on surface pressure. The enthalpy and entropy calculated from temperature-dependent isotherms clearly indicate the disordering effect of ILs. Further, the Gibbs free energy of mixing suggested the ILs to have attractive interaction with the lipid molecules, which is found to decrease with the surface pressure of the lipid film. This result is found to vary with the chain length of the ILs. The DSC thermograms of MLVs exhibit a sharp peak for pure lipid sample, which becomes very broad in the presence of IL. The shift of the peak position to lower temperature suggested the fluidizing effect of the IL.

## Materials and methods

### Materials

DPPC, 1-decyl-3-methylimidazolium tetrafluoroborate ([DMIM][BF4]), and 1-methyl-3-octylimidazolium tetrafluoroborate ([OMIM][BF4]) were purchased from Sigma-Aldrich (USA). Aqueous samples were prepared in de-ionized Millipore water (DI water) (resistivity ~ 18 MΩ cm) with pH ~ 7.0. The illustrative figures of [DMIM][BF4], [OMIM][BF4], and DPPC are shown in Fig. 1.

### Monolayer measurements

The pressure–area isotherms of zwitterionic lipid DPPC were measured by a Langmuir trough of size 55 × 15 × 0.5 $cm^3$ (APEX, India). The lipid solution (0.5 mg/mL in chloroform) was taken in a Hamilton syringe and 125 μL was spread uniformly over the de-ionized (DI) water surface of the trough. After the complete evaporation of chloroform (wait time ~ 15 min), the double barriers of the trough were symmetrically compressed at a fixed speed of 5 mm/min. An illustrative figure of the experimental setup is shown in Fig. 2. It is to be mentioned that, for the dynamic studies, the monolayers of pure lipids were initially compressed to a fixed surface pressure and then ILs were injected in the subphase. For the

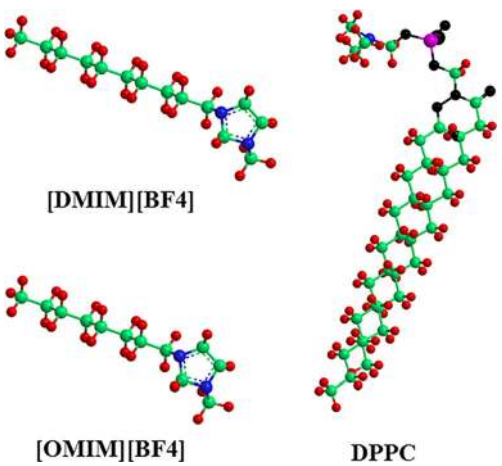


**Fig. 1** Structure of the chemicals used in the study

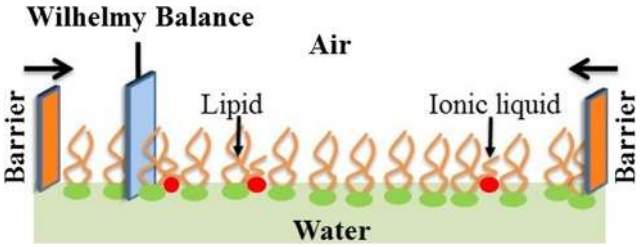


**Fig. 2** Schematic illustration of the experimental setup. The monolayer of lipid molecules is formed at the air–water interface by spreading the chloroform solution of the molecules. The interaction of ionic liquid in the lipid layer is monitored by measuring the thermodynamic parameters of the interactions (see text)

thermodynamic studies, the lipids and ILs were both dissolved in chloroform and then the solution of these mixtures was deposited on the water surface. To investigate the interaction of IL [DMIM][BF4] with DPPC lipid, the isotherms of the mixture of the lipid and IL were recorded. The temperature throughout the measurements was kept at 20 °C, with a fixed pH value of ~ 7.0. In order to prepare the binary solution, chloroform was used as a common solvent. For the kinetics of IL penetration into DPPC monolayer, the pure DPPC was spread over the water in the trough and the barriers were moved to a fixed surface pressure of 10 mN/m, 20 mN/m, and 30 mN/m. The barriers were kept stationary and for ~ 2 h for the film to equilibrate. Initially, there was a little drop in the surface pressure and, after some time, the pressure became stabilized. Then, about 300 μL of aqueous solution of [DMIM][BF4] (1 mg/mL stock solution) was injected in the subphase and the time evolution of surface pressure was monitored. Then, the relative change in surface pressure was calculated using the following equation, $\Delta\pi = \frac{\pi_f - \pi_0}{\pi_0}$, where $\pi_0$ and $\pi_f$ are the initial and final surface pressures, respectively. In order to find out the excess Gibbs free energy, the isotherms of pure DPPC and DPPC with [OMIM][BF4] or [DMIM][BF4] were recorded by following the above method. The concentration of added IL is defined as $\frac{[IL]}{[DPPC]+[IL]} x100\%$, where [IL] and [DPPC] are the number of moles of IL and DPPC, respectively. According to this definition, a sample represented in the following sections as 'DPPC/10 mol% [DMIM][BF4]' contains 0.1 mol fraction of [DMIM][BF4] in the mixtures of DPPC and [DMIM][BF4]. To measure the enthalpy and, consequently, entropy of monolayer systems, temperature-dependent area–pressure isotherms were measured using a KSV NIMA medium-sized trough equipped with two symmetrical barriers and a Wilhelmy balance. The temperature of the trough was varied and maintained using a JULABO FL300 temperature controller.

### DSC measurements

DSC measurements were performed on aqueous solution of DPPC MLVs (27 mg/mL) with and without 10 mol% [DMIM][BF4] using a Mettler Toledo DSC 3 STAR System. The thermograms were recorded for heating as well as cooling cycles with a scan rate of 0.5 °C/min within the temperature range 20–60°C. For MLV preparation, 5.4 mg dry DPPC was placed in a vial, to which chloroform/methanol solution (2:1 vol:vol) was added. The solution was bath sonicated for a couple of minutes. Then, it was dried under a stream of nitrogen. The vial was then placed in vacuum for about 12 h. A lipid thin film around the inner surface of the vial was formed. In case of pure DPPC MLV, about 0.2 mL of de-ionized (DI) water was added into the vial and vortexed to mix the film into solution, and then it was incubated at 50 °C for 1 h. In case of DPPC/[DMIM][BF4] sample, the IL was first added into the DI water and, then the aquous solution of the IL was added in the vial. The cycle of vortexing was repeated four to five times to obtain the final MLV solution.

## Results and discussion

### Penetration kinetics

To examine the effects of IL on DPPC monolayer formed at the air–water interface, the aqueous solution of IL was injected into the water subphase at a fixed surface pressure and the corresponding changes in surface pressure were monitored as a function of time. The insertion of the foreign molecules is reported to depend on the initial surface pressure of the lipid layer (Ghosh et al. 2010). Hence, the insertion ability of the [DMIM][BF4] into lipid monolayer has been monitored at three different initial surface pressures, namely, 10 mN/m, 20 mN/m, and 30 mN/m. The surface pressure–time curves for pure [DMIM][BF4] and DPPC/[DMIM][BF4] at these particular initial surface pressures are shown in Fig. 3. The variations are fitted with the Boltzmann-like equation:

$$\pi(t) = \frac{\pi_i - \pi_f}{1 + e^{\frac{t-t_0}{\tau}}} + \pi_f \quad (1)$$

where $\pi_i$ and $\pi_f$ are the initial and final surface pressures, respectively, time $t_0$ is the center value, and $\tau$ is the time constant. This constant provides a time scale for the time-dependent insertion of the IL into the lipid layer. For all initial surface pressures, IL solution was injected at about 4.0 cm away from the Wilhelmy plate. When the IL solution was injected into the subphase with no lipid molecules spread at the air–water interface, there was no change in the surface pressure with time. At 10 mN/m, the time constant from the fit is found to be 45 min, whereas for 20 mN/m, the value is 140 min. As evident, the time constant increases with increasing initial surface pressure. At higher initial surface pressure, the self-assembled lipid structure is compact compared to that of lower surface pressure and, thus, the IL takes longer time to penetrate into the monolayer. Note that, even after 12 h, there was no saturation in the

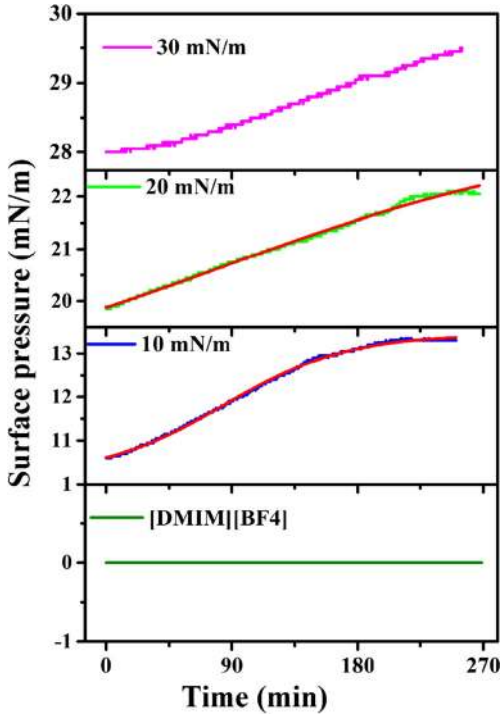


**Fig. 3** Variation of surface pressure of DPPC monolayer with [DMIM][BF4] injected in the subphase at initial surface pressures of 10mN/m, 20 mN/m, and 30 mN/m. The green line in the lower panel corresponds to the variation for only [DMIM][BF4] without lipid. The red lines for 10mN/m and 20 mN/m in second and third panels correspond to the fittings of the data

curve of 30 mN/m and, hence, the data were not fitted.

The percentage change in surface pressure ($\Delta\pi$) as a function of initial surface pressure is plotted in Fig. 4. From this figure, it is readily understood that, with the insertion of the IL, there is a substantial amount of increase in surface pressure. However, the changes vary inversely with the initial surface pressure. While at an initial pressure of 10 mN/m the increase is ~ 26%, the value drops to ~ 5% at an initial surface pressure of 30 mN/m over 4.5 h of observation. The findings from the evaluation of time constant and the increase in surface pressure suggest that there is a strong interaction between the lipid molecules and the IL. For the loosely bound lipid molecules at lower surface pressure, the IL can easily enter into the monolayer, resulting in a higher increase in surface pressure and the process is an accelerated one. On the other hand, it is difficult for the IL molecules to insert themselves when the lipid molecules are densely packed at higher surface pressure.

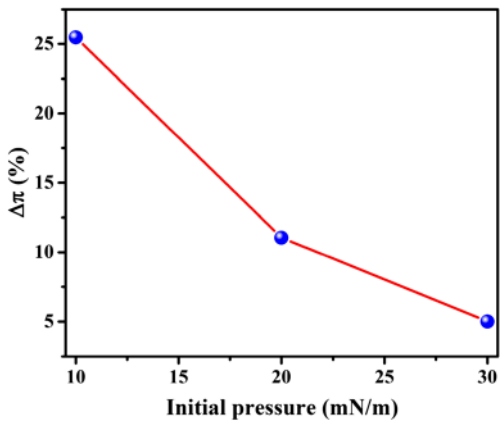


**Fig. 4** Relative changes in the surface pressure of DPPC monolayers with [DMIM][BF4] injected in the subphase at initial surface pressures of 10mN/m, 20mN/m, and 30 mN/m

As the surface pressure changes are only observed in the presence of lipids at the air–water interface, it is clear that the IL interacts strongly with the lipid monolayer. To obtain further insights into this interaction process, thermodynamical quantities have been measured, which are described in the following sections.

## Enthalpy and entropy

The surface pressure–area isotherms of monolayers of DPPC molecules formed at the air–water interface are shown in Fig. 5a, which are measured at different operating temperatures. At temperature ($T$) of 289 K, the isotherm does not exhibit any inflection point, which indicates that, even at around zero pressure, the condensed phase coexists with fluid phase. At $T > 289$ K, there is a prominent inflection point ($A_e$) at the beginning of a first-order phase transition where the disordered phase has been transformed into an ordered phase. The two-dimensional (2D) isothermal compressibility ($C_s$) can be evaluated from the same isotherms using (Giri et al. 2017a, b):

$$C_s = -\frac{1}{A}\left(\frac{\delta A}{\delta \pi}\right)_T \quad (2)$$

where $A$ is the mean molecular area and $\pi$ is the surface pressure at a given temperature ($T$). The evaluated values of $C_s$ (Eq. 2) for each isotherm is plotted in the inset of Fig. 5a. To ascertain the effect of the presence of the IL in the lipid monolayer, similar measurements were carried out for DPPC/[DMIM][BF4] (10 mol%) samples, and corresponding isotherms and $C_s$ are plotted in Fig. 5b. It is evident from the insets of these figures that there is a peak in $C_s$ at higher temperature, whereas at low temperature, it is almost flat. With increasing temperature, this peak position shifts to higher surface pressure, exhibiting the stability of LE phase. A similar effect of temperature is observed in the presence of IL in the monolayer. However, at a given temperature, the peaks are found to be broad in the presence of ILs, suggesting the effect of these ILs on the in-plane organization of the lipid molecules (Giri et al. 2017a, b). Actually, the peak in the compressibility of the pressure–area isotherm of a monolayer carry similar information to the enthalpy peak seen in the melting of a bilayer (Heimburg 2008). The enthalpy changes with and without the IL in the case of DPPC bilayer is

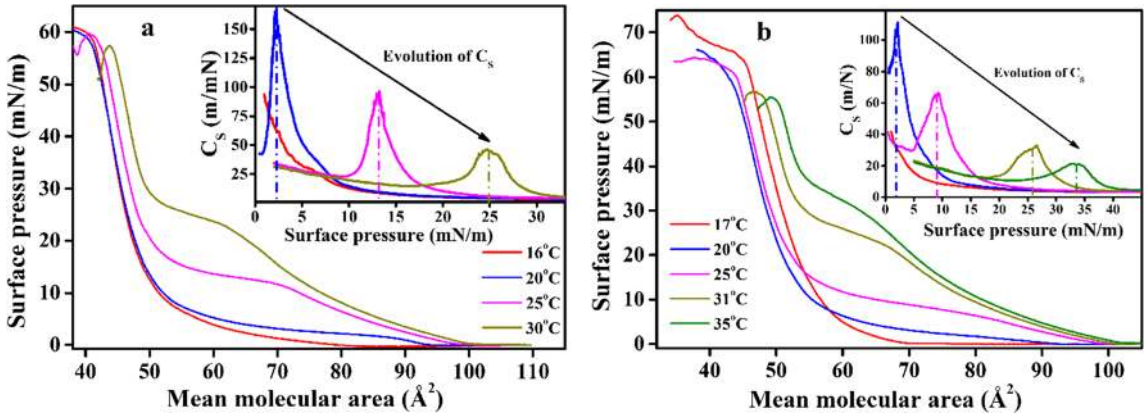


**Fig. 5** Pressure–area isotherms at different temperatures: **a** pure DPPC and **b** DPPC/10 mol% [DMIM][BF4]. The insets exhibit the corresponding 2D isothermal compressibility ($C_s$)

discussed later in this paper.

The thermodynamic transition between the disordered and ordered phases can be obtained from the kink point ($\pi_t$), which is the point of appearance of the ordered phase. The value of $\pi_t$ varies from isotherm to isotherm and the same has been plotted as a function of temperature in Fig. 6 for both DPPC and DPPC/10 mol% [DMIM][BF4] samples. An almost horizontal plateau is observed for both samples in temperature up to 303 K, beyond which the plateau starts to have a slope. At temperature $T \leq 288$ K, both the ordered and disordered phases are found to coexist, even at zero pressure. From these measurements, the change in enthalpy ($\Delta$H) during the phase transition can be calculated using the 2D Clausius–Clapeyron equation (Ni et al. 2006; Vollhardt and Brezesinski 2016):

$$\Delta H = (A_c - A_e) T \frac{d\pi_t}{dT} \tag{3}$$

where $A_e$ is the molecular area at the onset of the phase transition at surface pressure $\pi_t$ (as explained above) and $A_c$ is the area of the pure condensed phase (Vollhardt and Brezesinski 2016). $\frac{d\pi_t}{dT}$ is calculated from the slope of the curve of Fig. 6. The temperature-dependent enthalpies for both DPPC and DPPC/10 mol% [DMIM][BF4] are shown in Table 1. From the table, it is noteworthy to mention that, with the introduction of IL in the system, the enthalpy reduces significantly compared to the pure DPPC system. We further evaluated the temperature-dependent entropy change, $\Delta S = {}^{\Delta H}/_{T}$ for the phase transition, and this is plotted in Fig. 7. The negative $\Delta H$ and $\Delta S$ values signify the ordering in the system. As shown in the figure, the absolute values of $\Delta H$ and $\Delta S$ decrease with increasing temperature. One can also find that, around $T \sim 293$ K, $\Delta S$ for the pure DPPC system is around − 78 J/Kmol, whereas for DPPC/10 mol% [DMIM][BF4], the value reduces to around − 48 J/Kmol. The decrease in absolute value of the entropy as a function of added IL is observed at all the temperatures.

The value of entropy becomes less negative in the presence of IL compared to that of the pure DPPC system, which is correlated with the fact that the IL brings about a disordering effect in the self-assembled monolayer of DPPC. From this study, the strong perturbation in the self-assembled structure of the lipid monolayer due to interaction with IL is established.

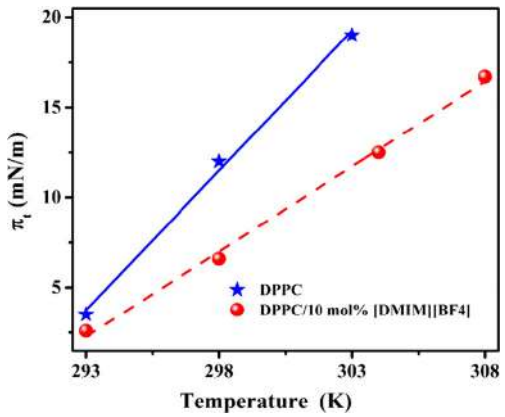


**Fig. 6** Variation of the main phase-transition pressure $\pi_t$ with temperature for DPPC (*blue solid line*) and DPPC/10 mol% [DMIM][BF4] (*red dash–dot line*) monolayers

## Miscibility and stability

To study the miscibility and stability of the binary mixture of DPPC and ILs with different chain lengths, the surface pressure–area isotherm data of monolayers for DPPC/[OMIM][BF4] and DPPC/[DMIM][BF4] formed at the air–water interface at 20

**Table 1** Change in enthalpy as a function of temperature for DPPC and DPPC/10 mol% [DMIM][BF4] monolayers

| Sample | Temperature (K) | Enthalpy (KJ/mol) |
|---|---|---|
| DPPC | 293 | − 22.9 |
| | 298 | − 18.9 |
| | 303 | − 15.9 |
| DPPC/10 mol% [DMIM][BF4] | 293 | − 14.0 |
| | 298 | − 11.9 |
| | 303 | − 10.9 |

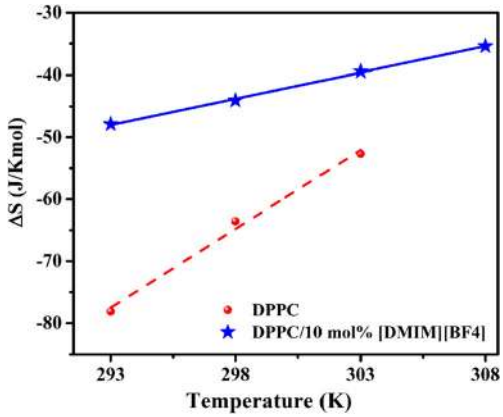


**Fig. 7** Temperature dependence of entropy change at the liquid extended (LE)/liquid condensed (LC) phase transition of DPPC monolayer (*red dash–dot line*) and DPPC/10 mol% [DMIM][BF4] (*blue solid line*) monolayers

°C were thermodynamically analyzed in Fig. 8a, b. For a given binary monolayer of two components, 1 and 2, the mean molecular area ($A_{12}$) of the mixed system would be the same or different to that of the total molecular area of the individual component 1 and 2. The miscibility of the two components can be obtained by calculating the excess mean molecular area ($\Delta A_{ex}$) of mixing, which is defined by (Gaines 1966; Davies and Jones 1992; Birdi 2013):

$$\Delta A_{ex} = A_{12} - (\chi_1 A_1 + \chi_2 A_2), \tag{4}$$

where $\chi_1$ and $\chi_2$ are the molar fractions of components 1 (lipid) and 2 (IL) and $A_1$ and $A_2$ are the molecular areas of pure lipid and pure IL at a given pressure and temperature. $\Delta A_{ex}$ will be zero for an ideal mixing of both components. A negative value corresponds to the interaction being attractive in nature. The calculated value of $\Delta A_{ex}$ from the isotherms of DPPC and ILs are shown in Fig. 9a, b for DPPC/[OMIM][BF4] and DPPC/[DMIM][BF4] with varying molar fraction of the respective ILs. As shown in the figure, the negative value of $\Delta A_{ex}$ implies that both the ILs are miscible in the DPPC monolayer (Hąc-Wydro et al. 2007; Wang et al. 2016).

At higher molar fraction, the value of $\Delta A_{ex}$ is found to be less negative. It is understood that the ILs here dissociate their $BF_4^-$ counterions into water, leaving the long chain cation in the lipid layer. Once some cationic part of ILs are mixed with the lipid layer, the layer possesses a net positive charge. Then, further inclusion of ILs into the layer becomes hard due to electrostatic repulsion between the lipid/IL film and the IL. Interestingly, the value of $\Delta A_{ex}$ becomes less negative at higher surface pressure, indicating a reduction in the miscibility. These results agree very well with the results obtained in independent measurements of the penetration kinetics of IL into lipid film discussed later.

To evaluate the thermodynamic stability of a mixture, the excess Gibbs free energy ($\Delta G_{ex}$) can be calculated from the excess mean molecular area ($\Delta A_{ex}$) (Wang et al. 2016). This excess energy is the difference in Gibbs free energies between a real and an ideal mixture, which are measured at a specific surface pressure and a constant temperature. Excess Gibbs free energy can be calculated as (Sabatini et al. 2008):

$$\Delta G_{ex} = \int_0^{\pi} (A_{12} - (\chi_1 A_1 + \chi_2 A_2) d\pi \tag{5}$$

The negative value of $\Delta G_{ex}$ calculated using Eq. 5 indicates a net attraction between the two components that produces stability. From Fig. 10a, b, one can see that, for $\chi_2 > 0.1$, the $\Delta G_{ex}$ values become less negative, which implies that the films become less stable in nature. As shown by the results in the figures, in the case of $\chi_2 = 0.2$, at 25 mN/m surface pressure, the value of $\Delta G_{ex}$ is − 535 J/mol for [OMIM][BF4], while for [DMIM][BF4], the value is − 452 J/mol. As the $\Delta G_{ex}$ is less negative for [DMIM][BF4] compared to [OMIM][BF4], it is conclusive that the effect of longer chains is more lethal than that of the shorter chains. Note that [DMIM][BF4] has 10 carbons in the hydrophobic chain, while

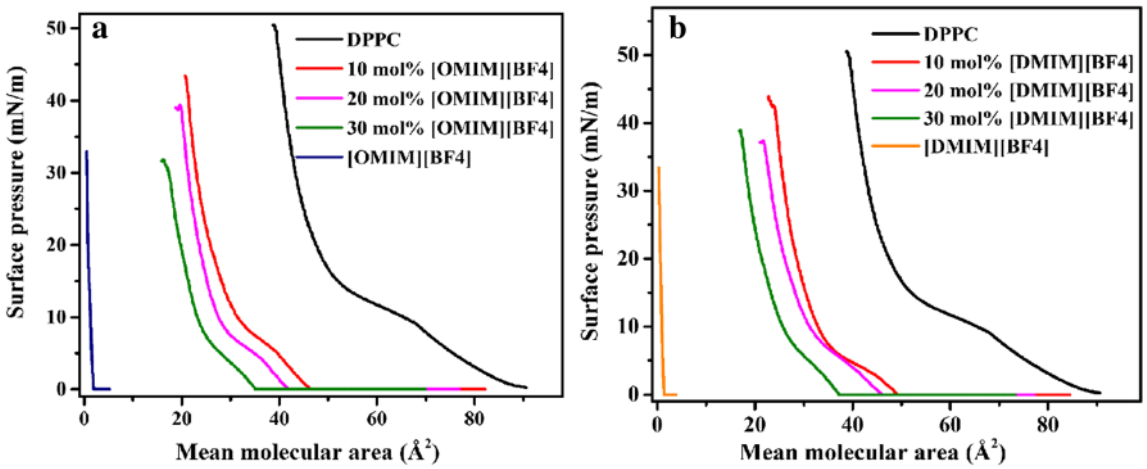


**Fig. 8** Pressure–area isotherms of the DPPC monolayer with different molar % of **a** [OMIM][BF4] and **b** [DMIM][BF4]

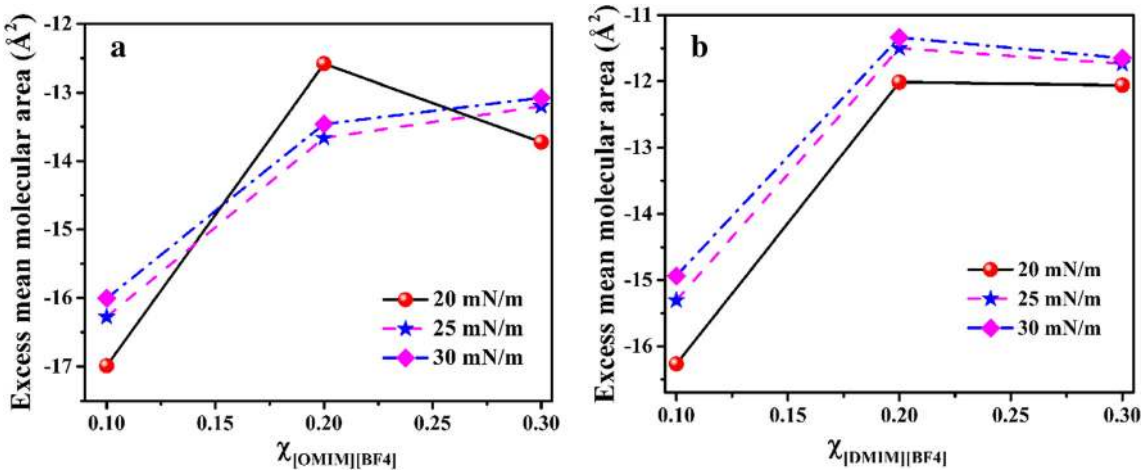


**Fig. 9** Variation of excess mean molecular area ($\Delta A_{ex}$) for **a** DPPC/[OMIM][BF4] and **b** DPPC/[DMIM][BF4] with molar fraction at various constant surface pressures and at a constant temperature of 295 K

[OMIM][BF4] has 8. The trend remains similar for three different surface pressures; however, at lower surface pressure, the effect is stronger. This can be correlated with the fact that it is easier for the ILs to penetrate into the monolayer at lower surface pressure, where lipid molecules are relatively further apart from each other.

All the above measurements and derived results suggest that the ILs interact strongly with the lipid monolayer and these interactions can be quantified by corresponding changes in enthalpy, entropy, and Gibbs free energy. We know that biological cell membranes are made up of two such monolayers fetching each other to form a bilayer. Hence, to investigate the effect of IL on a prototype cellular membrane, a DSC study on an MLV with and without IL was carried out.

## DSC measurements

DSC measurement was carried out to find out the impact of [DMIM][BF4] on the thermotropic phase behavior of DPPC lipids in the MLV structure. In the present study, 10 mol% of the IL has been used in DPPC lipids to form these MLVs. The corresponding thermograms are shown in Fig. 11 for both heating and cooling cycles. Pure DPPC membrane shows a sharp peak at ~ 41.5°C, which corresponds to the main phase transition (gel to fluid). Generally, the DSC thermograms of DPPC vesicles show a pretransition peak corresponding to the melting of the ripple phase. The position and intensity of this peak depend on many factors, such as the ionic strength of solvent, impurity of lipids, and sample preparation conditions. In the data analysis process, background subtraction plays an important role in resolving such a peak. In the present study, the absence of this peak may be a consequence of one or all of these reasons. In the sample with 10 mol% [DMIM][BF4] in the lipid vesicles, the main peak has shifted towards lower temperature, at around ~ 38 °C. A similar effect has been seen in the case of melting of the 1,2-dimyristoyl-sn-glycero-3-phosphorylcholine (DMPC) bilayer with the same IL (Sharma et al. 2017). The decrease in the phase transition

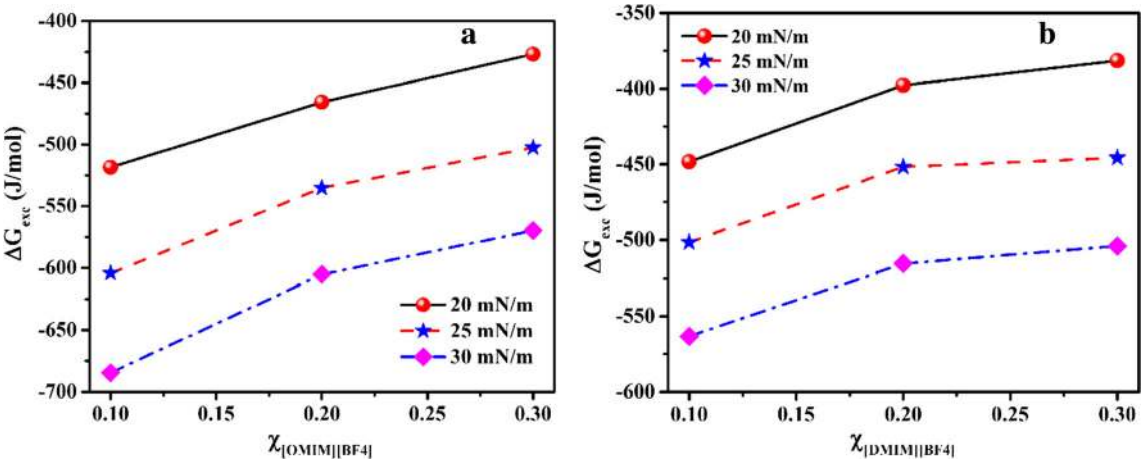


**Fig. 10** Variation of excess Gibbs free energy ($\Delta G_{ex}$) for **a** DPPC/[OMIM][BF4] and **b** DPPC/[DMIM][BF4] with molar fraction at various constant surface pressures and temperature of 295 K

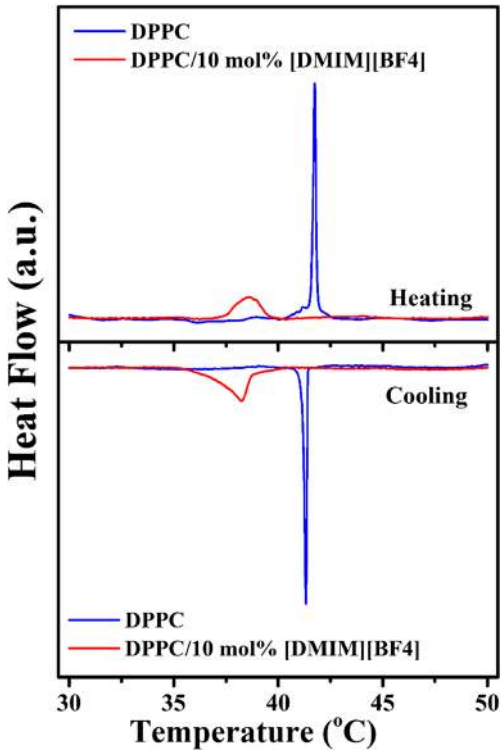


**Fig. 11** DSC thermograms of DPPC vesicles with and without [DMIM][BF4] in heating and cooling cycles

temperature portrays the fact that the IL fluidizes the lipid membrane. Further, the peak becomes broadened due to IL, which is a similar effect observed in the in-plane compressibility of the lipid layer. It suggests the IL to have the same effect in disordered to ordered transition in the lipid monolayer as a function of surface pressure and the fluid to gel transition in the lipid bilayer as a function of temperature. The calculated enthalpy change ($\Delta H$) for the transition in the DPPC sample is found to be around − 1.00 J/g, while for the sample with IL, it is around − 0.53 J/g. Low thermal energy required for the observed gel–fluid transition suggests a disordering effect of the IL in the lipid membrane. Interestingly, a recent publication by Wang et al. (2016) found this disordering effect to be a function of hydrophobic chain length of the added molecules. In fact, an opposite result was found in the case of imidazolium-based lipid analog with 15 carbons in the chain. A more systematic DSC measurement is required by altering the lipid compositions of the vesicles as well as the chain length and anionic and cationic parts of ILs. This may provide a better description of the thermodynamics of IL–membrane interactions.

## Conclusion

Different thermodynamic parameters evaluated from the area–pressure isotherms of lipid monolayer suggest a strong effect of ionic liquids (ILs) on the organization of lipid molecules in the layer. The imidazolium-based ILs with 8 and 10 carbons in their hydrocarbon chains exhibit a disordering effect that is found to vary with surface pressure of the monolayer and the chain lengths of ILs. Similar results have been observed for lipid bilayers. The effect of ILs observed in a living organism may be because of interaction with cellular membrane or with the cytoplasmic components of the cell or a combination of both. However, as all the ILs are organic compounds and amphiphilic in nature, they are expected to affect the structure of cellular membrane. In the present study, the ILs, being with a positively charged large molecule, insert their hydrocarbon chain into the lipid layer due to the favorable hydrophobic interaction, whereas the small anions are expected to dissociate into the bulk water. The insertion of the cation may exert a lateral push to the lipid chains that causes the lipid molecules to disorder. Such an interaction can also increase the conformational entropy of the lipid molecules. As discussed, the lipid bilayer in a cellular membrane has its own self-assembled structure to accomplish the assigned physiological functions. Any perturbation from this specific structure may lead to malfunctioning of the membrane, causing the cell to die. In fact, the favorable interaction, as explained in this present work, between IL and lipid membrane bring considerable structural changes, which have been quantified in our earlier work (Bhattacharya et al. 2017) and also reported by others (Benedetto 2017). Even though these simple approaches used in the present study offered very important information about the interaction of ILs with lipid membrane, a more systematic study with different experimental and simulation techniques are required to shed light on the detailed mechanism of functioning of ILs on living organisms.

In the present study, only imidazolium-based IL has been used to investigate the interaction with a zwitterionic lipid membrane. The biological membranes are compositionally much more complicated. To mimic the system better, one should consider a multicomponent system with varying lipid heads (PC, PE, or other group, few mole percent of negatively or positively charged head group in the presence of zwitterionic one) and chains (different chain lengths or saturated and unsaturated chains). As the field of IL is very rich, one has to investigate the effect by varying these molecules also. For example, one could use ammonium-based ILs to shed light on the issue of less toxicity of these molecules compared to the imidazolium-based ILs. In the future, all such facets of the IL–membrane interactions have to be explored by measuring the thermodynamic parameters to achieve a general description of the interaction.

**Acknowledgements** SKG acknowledges the financial support received from UGC-DAE CSR (Mumbai Centre). We acknowledge the scientific discussions with Dr. P. Munshi and Dr. M. K. Mukhopadhyay.

## Compliance with ethical standards

**Conflict of interest** G. Bhattacharya declares that he has no conflict of interest. S. Mitra declares that she has no conflict of interest. P. Mandal declares that she has no conflict of interest. S. Dutta declares that he has no conflict of interest. R. P. Giri declares that he has no conflict of interest. S. K. Ghosh declares that he has no conflict of interest.

**Ethical approval** This article does not contain any studies with human participants or animals performed by any of the authors.

## References


Aroti A, Leontidis E, Maltseva E, Brezesinski G (2004) Effects of Hofmeister anions on DPPC Langmuir monolayers at the air–water interface. J Phys Chem B 108(39):15238–15245

Babalola GO (1998) Anti-bacterial activity of synthetic N-heterocyclic oxidizing compounds. Lett Appl Microbiol 26(1):43–46

Benedetto A (2017) Room-temperature ionic liquids meet bio-membranes: the state-of-the-art. Biophys Rev 9(4):309–320

Benedetto A, Heinrich F, Gonzalez MA, Fragneto G, Watkins E, Ballone P (2014) Structure and stability of phospholipid bilayers hydrated by a room-temperature ionic liquid/water solution: a neutron reflectometry study. J Phys Chem B 118(42):12192–12206

Benedetto A, Bingham RJ, Ballone P (2015) Structure and dynamics of POPC bilayers in water solutions of room temperature ionic liquids. J Chem Phys 142:124706

Bhattacharya G, Giri RP, Saxena H, Agrawal VV, Gupta A, Mukhopadhyay MK, Ghosh SK (2017) X-ray reflectivity study of the interaction of an imidazolium-based ionic liquid with a soft supported lipid membrane. Langmuir 33(5):1295–1304

Bingham RJ, Ballone P (2012) Computational study of room-temperature ionic liquids interacting with a POPC phospholipid bilayer. J Phys Chem B 116(36):11205–11216

Birdi KS (2013) Lipid and biopolymer monolayers at liquid interfaces. Plenum Press, New York

Blume A (1983) Apparent molar heat capacities of phospholipids in aqueous dispersion. Effects of chain length and head group structure. Biochemistry 22(23):5436–5442

Byrne N, Angell CA (2009) Formation and dissolution of hen egg white lysozyme amyloid fibrils in protic ionic liquids. Chem Commun 9: 1046–1048

Davies RJ, Jones MN (1992) The thermal behaviour of phosphatidylcholine–glycophorin monolayers in relation to monolayer and bilayer internal pressure. Biochim Biophys Acta Biomembr 1103(1):8–12

DiCarlo CM, Compton DL, Evans KO, Laszlo JA (2006) Bioelectrocatalysis in ionic liquids. Examining specific cation and anion effects on electrode-immobilized cytochrome c. Bioelectrochemistry 68(2):134–143

Docherty KM, Kulpa CF Jr (2005) Toxicity and antimicrobial activity of imidazolium and pyridinium ionic liquids. Green Chem 7(4):185–189

Drücker P, Rühling A, Grill D, Wang D, Draeger A, Gerke V, Glorius F, Galla H-J (2017) Imidazolium salts mimicking the structure of natural lipids exploit remarkable properties forming lamellar phases and giant vesicles. Langmuir 33(6):1333–1342

Evans KO (2008) Supported phospholipid bilayer interaction with components found in typical room-temperature ionic liquids—a QCM-D and AFM study. Int J Mol Sci 9(4):498–511

Frade RF, Matias A, Branco LC, Afonso CA, Duarte CM (2007) Effect of ionic liquids on human colon carcinoma HT-29 and CaCo-2 cell lines. Green Chem 9(8):873–877

Gaines GL (1966) Thermodynamic relationships for mixed insoluble monolayers. J Colloid Interface Sci 21(3):315–319

Gayet F, Marty JD, Brûlet A, Viguerie NL (2011) Vesicles in ionic liquids. Langmuir 27(16):9706–9710

Ghosh SK, Castorph S, Konovalov O, Jahn R, Holt M, Salditt T (2010) In vitro study of interaction of synaptic vesicles with lipid membranes. New J Phys 12(10):105004

Ghosh SK, Castorph S, Konovalov O, Salditt T, Jahn R, Holt M (2012) Measuring Ca2+-induced structural changes in lipid monolayers: implications for synaptic vesicle exocytosis. Biophys J 102(6): 1394–1402

Giehl A, Lemm T, Bartelsen O, Sandhoff K, Blume A (1999) Interaction of the GM2-activator protein with phospholipid–ganglioside bilayer membranes and with monolayers at the air–water interface. FEBS J 261(3):650–658

Giri RP, Chakrabarti A, Mukhopadhyay MK (2017a) Cholesterol-induced structural changes in saturated phospholipid model membranes revealed through X-ray scattering technique. J Phys Chem B 121(16):4081–4090

Giri RP, Mukhopadhyay MK, Mitra M, Chakrabarti A, Sanyal MK, Ghosh SK, Bera S, Lurio LB, Ma Y, Sinha SK (2017b) Differential adsorption of a membrane skeletal protein, spectrin, in phospholipid membranes. Europhys Lett 118(5):58002

Gorman-Lewis DJ, Fein JB (2004) Experimental study of the adsorption of an ionic liquid onto bacterial and mineral surfaces. Environ Sci Technol 38(8):2491–2495

Hąc-Wydro K, Wydro P, Jagoda A, Kapusta J (2007) The study on the interaction between phytosterols and phospholipids in model membranes. Chem Phys Lipids 150(1):22–34

Hallett JP, Welton T (2011) Room-temperature ionic liquids: solvents for synthesis and catalysis. 2. Chem Rev 111(5):3508–3576

Heimburg T (2008) Thermal biophysics of membranes. Wiley, Weinheim

Jurak M (2013) Thermodynamic aspects of cholesterol effect on properties of phospholipid monolayers: Langmuir and Langmuir–Blodgett monolayer study. J Phys Chem B 117(13):3496–3502

Kalhor HR, Kamizi M, Akbari J, Heydari A (2009) Inhibition of amyloid formation by ionic liquids: ionic liquids affecting intermediate oligomers. Biomacromolecules 10(9):2468–2475

Kelman D, Kashman Y, Rosenberg E, Ilan M, Ifrach I, Loya Y (2001) Antimicrobial activity of the reef sponge Amphimedon viridis from the red sea: evidence for selective toxicity. Aquat Microb Ecol 24(1): 9–16

Kontro I, Svedström K, Duša F, Ahvenainen P, Ruokonen S-K, Witos J, Wiedmer SK (2016) Effects of phosphonium-based ionic liquids on phospholipid membranes studied by small-angle X-ray scattering. Chem Phys Lipids 201:59–66

Kulacki KJ, Lamberti GA (2008) Toxicity of imidazolium ionic liquids to freshwater algae. Green Chem 10(1):104–110

Kumar RA, Papaïconomou N, Lee JM, Salminen J, Clark DS, Prausnitz JM (2009) In vitro cytotoxicities of ionic liquids: effect of cation rings, functional groups, and anions. Environ Toxicol 24(4):388–395

Laszlo JA, Compton DL (2002) Comparison of peroxidase activities of hemin, cytochrome c and microperoxidase-11 in molecular solvents and imidazolium-based ionic liquids. J Mol Catal B 18(1):109–120

Li G, Shen J, Zhu Y (1998) Study of pyridinium-type functional polymers. II. Antibacterial activity of soluble pyridinium-type polymers. J Appl Polym Sci 67(10):1761–1768

Lim GS, Zidar J, Cheong DW, Jaenicke S, Klähn M (2014) Impact of ionic liquids in aqueous solution on bacterial plasma membranes studied with molecular dynamics simulations. J Phys Chem B 118(35):10444–10459

Lombard J (2014) Once upon a time the cell membranes: 175 years of cell boundary research. Biol Direct 9(1):32

Mikkola S-K, Robciuc A, Lokajova J, Holding AJ, Lämmerhofer M, Kilpeläinen I, Holopainen JM, King AW, Wiedmer SK (2015)

Impact of amphiphilic biomass-dissolving ionic liquids on biological cells and liposomes. Environ Sci Technol 49(3):1870–1878

Nakahara H, Hagimori M, Mukai T, Shibata O (2016) Interactions of a tetrazine derivative with biomembrane constituents: a Langmuir monolayer study. Langmuir 32(26):6591–6599

Ni S, Lee W, Li B, Esker AR (2006) Thermodynamics of the liquid expanded to condensed phase transition of poly(L-lactic acid) in Langmuir monolayers. Langmuir 22(8):3672–3677

Petelska AD, Figaszewski ZA (2011) The equilibria of lipid–K+ ions in monolayer at the air/water interface. J Membr Biol 244(2):61–66

Ranke J, Müller A, Bottin-Weber U, Stock F, Stolte S, Arning J, Störmann R, Jastorff B (2007) Lipophilicity parameters for ionic liquid cations and their correlation to in vitro cytotoxicity. Ecotoxicol Environ Saf 67(3):430–438

Rogers RD, Plechkova NN, Seddon KR (2009) Ionic liquids: from knowledge to application. ACS Symposium Series, vol 1030. American Chemical Society, Washington

Russo G, Witos J, Rantamäki AH, Wiedmer SK (2017) Cholesterol affects the interaction between an ionic liquid and phospholipid vesicles. A study by differential scanning calorimetry and nanoplasmonic sensing. Biochim Biophys Acta Biomembr 1859(12):2361–2372

Sabatini K, Mattila J-P, Kinnunen PK (2008) Interfacial behavior of cholesterol, ergosterol, and lanosterol in mixtures with DPPC and DMPC. Biophys J 95(5):2340–2355

Sharma VK, Ghosh SK, Mandal P, Yamada T, Shibata K, Mitra S, Mukhopadhyay R (2017) Effects of ionic liquids on the nanoscopic dynamics and phase behaviour of a phosphatidylcholine membrane. Soft Matter 13(47):8969–8979

Smiglak M, Pringle JM, Lu X, Han L, Zhang S, Gao H, MacFarlane DR, Rogers RD (2014) Ionic liquids for energy, materials, and medicine. Chem Commun 50(66):9228–9250

Vollhardt D, Brezesinski G (2016) Phase characteristics of 1-monopalmitoyl-rac-glycerol monolayers at the air/water interface. Langmuir 32(29):7316–7325

Wang D, de Jong DH, Rühling A, Lesch V, Shimizu K, Wulff S, Heuer A, Glorius F, Galla H-J (2016) Imidazolium-based lipid analogues and their interaction with phosphatidylcholine membranes. Langmuir 32(48):12579–12592

Weaver KD, Van Vorst MP, Vijayaraghavan R, MacFarlane DR, Elliott GD (2013) Interaction of choline salts with artificial biological membranes: DSC studies elucidating cellular interactions. Biochim Biophys Acta Biomembr 1828(8):1856–1862

Yoo B, Shah JK, Zhu Y, Maginn EJ (2014) Amphiphilic interactions of ionic liquids with lipid biomembranes: a molecular simulation study. Soft Matter 10(43):8641–8651

Yoo B, Zhu Y, Maginn EJ (2016) Molecular mechanism of ionic-liquid-induced membrane disruption: morphological changes to bilayers, multilayers, and vesicles. Langmuir 32(21):5403–5411

Yu Y, Nie Y (2011) Toxicity and antimicrobial activities of ionic liquids with halogen anion. J Environ Prot 2(03):298–303